Proceedings of 13th International Heat Transfer Conference, Sydney, Australia, August 13-18, 2006
Paper No. MPH-46

TWO-PHASE FLOW SIMULATION OF MIST FILM COOLING WITH DIFFERENT WALL HEATING CONDITIONS

Xianchang Li and Ting Wang
Energy Conversion and Conservation Center
University of New Orleans
New Orleans, Louisiana, USA

Abstract

Effective cooling of gas turbine combustor liners, combustor transition pieces, turbine vanes (nozzles) and blades (buckets) is a critical task to protect these components from the flue gas at extremely high temperature. Air film cooling has been successfully used to cool these hot sections for the last half century. However, the net benefits from the traditional methods seem to be marginally incremental, but the temperature of working gas is continuously increasing to achieve a high thermal efficiency. Therefore, new cooling techniques need to be developed. One of the promising techniques is to enhance film cooling with mist injection. While the previous study reported the effect of mist on the cooling effectiveness with an adiabatic wall, this paper focuses on the effect of mist injection on heat transfer of film cooling with a non-adiabatic flat wall, using commercial CFD software package Fluent. Both 2-D and 3-D cases are considered with a 2-D slot and diffusive compound angle holes. Modellings of interaction of droplet with uniformly cooled wall as well as conjugate heat conduction inside the solid base are conducted. Different mist droplet sizes and mist concentrations are adopted. Both conditions at a gas turbine operating environment (15 atm and 1561K) and in the laboratory environment (1 atm and 450K) are considered. Results show that injecting 2~10% mist successfully reduces the heat transfer coefficient and the wall temperature. Especially, mist has the prolonged effect of cooling the region downstream of 15 jet hole diameters, where the conventional air film cooling is not effective.

Nomenclature

b	slot width (m)
C	concentration (kg/m^3)
d	diameter (m)
GT	gas turbine
k	turbulence kinetic energy (m^2/s^2)
k_c	mass transfer coefficient (m/s)
M	blowing ratio, $(\rho u)_c/(\rho u)_g$
q_w"	wall heat flux
S	source term
Tu	turbulence intensity

Greek

ε	turbulence dissipation rate (m^2/s^3)
η_a	adiabatic film cooling effectiveness, $(T_g-T_{aw})/(T_g-T_c)$
λ	thermal conductivity (W/m-K)

Subscript

aw	adiabatic wall
c	coolant or jet flow
i	internal cooling
p	particle or droplet

1. Introduction

To improve the thermal efficiency of gas turbines, the turbine inlet temperature (TIT) is usually elevated higher than the metal melting point. Effective cooling of gas turbine combustor liners, combustor transition pieces, turbine vanes (nozzles) and blades (buckets) is a critical task to protect these components from the hot flue gas. Air film cooling as well as airfoil internal cooling have

been successfully used in gas turbine applications for the last half-century. To make the cooling more effective, significant effort and research have been conducted. Many flow and geometric parameters affect the performance of film cooling, such as jet hole shape and coolant injection angle, blowing ratio, inlet velocity profile, turbulence intensity, coolant-supply plenum configuration, etc. These parameters have to be optimized to achieve good cooling performance (Brittingham and Leylek, 2002, Jia et al. 2003). For example, the injection angle is mostly less than 35^o to reduce the jet separation and flow recirculation. Studies also found that lateral or forward diffusive holes perform better than simple forward hole. A well-designed diffusive hole can mimic the performance of a slot jet (Brittingham and Leylek, 2002). Turbulence intensity can either upgrade or downgrade film-cooling performance depending on the blowing ratio and flow structure (Mayhew et al., 2004). Further studies have also been conducted on some specific parameters, such as the effect of surface roughness on film cooling (Rutledge et al., 2005) and the cooling of trailing edge cut-back (Martini et al., 2005).

Selection and validation of turbulence modellings is vital to predict film-cooling performance. Turbulence models adopted include V2F k-ε by Jia et al. (2003), the standard k-ε model by Brittingham and Leylek (2002), k-ω model by Heidmann et al. (2000), and large eddy simulation (LES) by Tyagi and Acharya (2003). In general, numerical simulation can provide ideal boundary conditions but may fail to accurately predict the flow separation and correct physics.

Film cooling technology has become quite mature during the development of the past five decades. The net benefits from further improvement seem to be marginally incremental. New cooling techniques need to be developed to surpass the current limits. To this end, this paper proposes to simulate injecting water mist into the air coolant to improve the film cooling performance. By injecting water mist into the coolant flow, each droplet acts as a heat sink. Droplet evaporation reduces the flow temperature near the surface and thus provides a better protection for the surface. The cooling effectiveness can also be enhanced due to direct contacts between droplets and the wall. Other enhancing mechanisms include high temperature gradient near the wall, augmented mixing by droplet-air interactions, and increased specific heat. In addition, the residence time needed for droplet evaporation postpones the enhancement into downstream region where single-phase air film cooling becomes less powerful. By taking the advantage of the aforementioned heat transfer mechanisms, mist has been employed in gas turbine inlet air fog cooling (Chaker et al., 2002), overspray cooling through wet compression (Petr et al., 2003), and airfoil internal cooling (Guo and Wang, 2000).

Li and Wang (2005a, 2005b) evaluated the effect of mist injection on film cooling with numerical simulation under low temperature, velocity and pressure. It was shown that a small amount of mist injection (2% of the coolant mass flow rate) could increase the adiabatic cooling effectiveness about 30% ~ 50%. Further study indicated that smaller droplets and higher mist concentration result in a better enhancement. Afterwards, Wang and Li (2006) examined the performance of mist film cooling under gas turbine operational conditions, feathered by high pressure (15 atm), velocity (128 m/s), and temperature (1561k). The enhancement of the adiabatic cooling effectiveness was found less attractive than the cases with low pressure, velocity and temperature conditions. However, due to high surface temperature under the GT operating condition, the additional wall temperature reduction could achieve 60K even though the enhancement of adiabatic cooling effectiveness is only 5%. This temperature reduction can be critical to the airfoil life expectancy of gas turbines.

Previous studies (Li and Wang, 2005a, 2005b, Wang and Li, 2006) reported only the effect of mist on the adiabatic cooling effectiveness. As a continuation of mist film cooling study, this paper focuses on mist film cooling heat transfer coefficient with a **non-adiabatic surface**. A 2-D slot and 3-D diffusive compound-angle holes are considered in this study with both a uniformly cooled wall at a constant heat flux and a conjugate inner wall cooling by an internal cooling flow.

2. Numerical Model

2.1 Geometric Configurations and Physical Model

Recognizing that a diffusive compound-angle hole generally provides a good cooling performance, it is employed first in this study. Figure 1 shows the details of the diffusive compound angle hole. The forward angle is 35° with an extra diffusive angle of 15°, and the inclination angle in the direction perpendicular to the mainstream is 30°. The nominal diameter (d) of the injection hole is 1 mm. The vertical height of the jet hole is 1.72d, which gives an actual jet hole length of 3d. The computational domain is 40d in the mainstream direction and 3d in the spanwise direction. The domain has a height of 10d. The distance between the mainstream inlet and the coolant jet injection hole is 10d.

To more closely simulate the real turbine airfoils cooling including both the external film and the internal channel flow cooling, a 2-D slot with a slot width (b) of 4 mm is employed as shown in Figure 1. The slot width is chosen to be consistent with previous studies. In this conjugate cooling arrangement, the solid metal wall with a uniform thickness of 1.72d is included in the computational domain. Below the base wall bottom surface, an internal cooling channel flow is imposed with an internal heat transfer coefficient h_i and a coolant flow temperature T_{ci}.

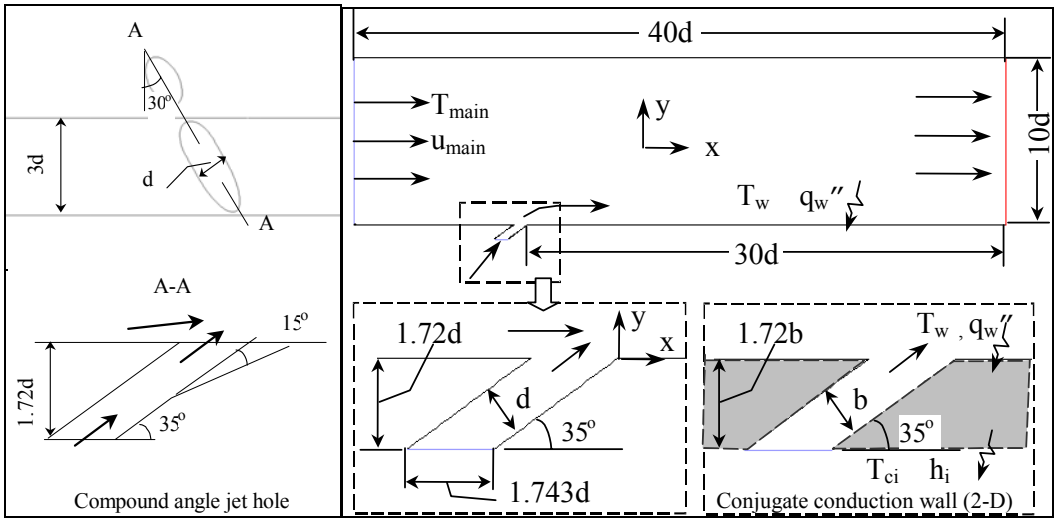

Figure 1 Computational domain and cooling hole configurations

A feasible method to simulate the film cooling with mist injection is to consider the droplets as a discrete phase since the volume fraction of the liquid is usually small (less than 1%). The trajectories of the dispersed phase (droplets) are calculated by the Lagrangian method. The impacts of the droplets on the continuous phase are considered as source terms to the governing equations of mass, momentum, energy and species equations. Three species (oxygen, nitrogen and water vapor) are simulated in mist film cooling flow. The standard k-ε model is used with enhanced near-wall treatment to the continuous phase (air). The governing equations as well as the turbulence model are summarized in Table 1.

The droplet trajectory is traced by applying the Newton's 2nd Law. The energy balance for each droplet can be given as

$$m_p c_p \frac{dT}{dt} = \pi d^2 h_d (T_\infty - T) + \frac{dm_p}{dt} h_{fg} \qquad (1)$$

Table 1 Governing Equations and k-ε Turbulence Model

$\frac{\partial}{\partial x_i}(\rho u_i) = S_m$	$\frac{\partial}{\partial x_i}(\rho u_i k) = \frac{\partial}{\partial x_i}\left[\left(\mu + \frac{\mu_t}{\sigma_k}\right)\frac{\partial k}{\partial x_i}\right] + G_k - \rho\varepsilon$
$\frac{\partial}{\partial x_i}(\rho u_i u_j) = \rho\bar{g}_j - \frac{\partial P}{\partial x_j} + \frac{\partial}{\partial x_i}\left(\tau_{ij} - \rho\overline{u'_i u'_j}\right) + F_j$	$\frac{\partial}{\partial x_i}(\rho u_i \varepsilon) = \frac{\partial}{\partial x_i}\left[\left(\mu + \frac{\mu_t}{\sigma_\varepsilon}\right)\frac{\partial \varepsilon}{\partial x_i}\right] + C_{1\varepsilon}G_k\frac{\varepsilon}{k} - C_{2\varepsilon}\rho\frac{\varepsilon^2}{k}$
$\frac{\partial}{\partial x_i}(\rho c_p u_i T) = \frac{\partial}{\partial x_i}\left(\lambda\frac{\partial T}{\partial x_i} - \rho c_p\overline{u'_i T'}\right) + \mu\Phi + S_h$	$\mu_t = \rho C_\mu \frac{k^2}{\varepsilon}$
	$\lambda_{eff} = \lambda + c_p\mu_t / Pr_t$
$\frac{\partial}{\partial x_i}(\rho u_i C_j) = \frac{\partial}{\partial x_i}\left(\rho D_j\frac{\partial C_j}{\partial x_i} - \rho\overline{u'_i C'_j}\right) + S_j$	$D_{eff} = D + \mu_t / Sc_t$

where h_{fg} is the latent heat. The convective heat transfer coefficient (h_d) can be obtained with an empirical correlation (Ranz and Marshall, 1952). The mass change rate/vaporization rate (dm_p/dt) is governed by concentration difference between droplet surface and air stream.

$$-\frac{dm_p}{dt} = \pi d^2 k_c (C_s - C_\infty) \tag{2}$$

where k_c is the mass transfer coefficient, C_s is the vapor concentration at droplet surface, and C_∞ is the vapor concentration of the bulk flow. When the droplet temperature reaches the boiling point, its evaporation rate will be evaluated by (Kuo, 1986):

$$-\frac{dm_p}{dt} = \pi d^2\left(\frac{\lambda}{d}\right)(2.0 + 0.46 Re_d^{0.5}) \ln\left(1 + c_p(T_\infty - T)/h_{fg}\right)/c_p \tag{3}$$

where λ is the gas/air heat conductivity, and c_p is its specific heat.

Stochastic method is used to consider the effect of turbulence dispersion on droplets tracking. The droplet trajectories are calculated with the instantaneous flow velocity ($\bar{u} + u'$), and the velocity fluctuations are then given as:

$$u' = \varsigma\left(\overline{u'^2}\right)^{0.5} = \varsigma(2k/3)^{0.5} \tag{4}$$

where ς is a normally distributed random number. This velocity will apply during the characteristic lifetime of the eddy (t_e), a time scale calculated from the turbulence kinetic energy and dissipation rate. After this time period, the instantaneous velocity will be updated with a new ς value until a full trajectory is obtained. More numerical details are given in Fluent (2005).

2.2 Boundary Conditions and Operational Parameters

To explore the physics of mist film cooling under a real GT operating environment, simulation needs to be conducted under high-pressure and high-temperature conditions, which is difficult and expensive for experimental studies. The parameters simulating the GT operating environment are listed in Table 2 (3-D case). Note these parameters represent a general condition in a F-frame type GT without trying to match the specific condition of any brand or model. Periodic boundary condition is assigned in the spanwise direction. All other walls are adiabatic and have a non-slip velocity boundary condition. Also listed in Table 2 are another set of 2-D slot flow conditions with low temperature, pressure, and velocity for typical laboratory experiments that are similar to those used in many other literatures. For the 2-D conjugate cases, the solid wall is assumed to be alloy

steel with a density of 8030 kg/m^3, heat conductivity of 16.27 W/m-K, and specific heat of 502 J/kg-K. A heat transfer coefficient of h_i = 20 W/m^2-K and internal coolant flow temperature T_{ci} = 375K are assigned to the internal cooling flow, which is located at the bottom of Figure 1. For a convenient comparison with the 3-D case, the boundary condition of a constant cooling flux is also assigned to the 2-D case.

Table 2 Parameters used in simulation for different cases

		3-D hole	2-D hole	
Operational pressure	P (atm)	15	1	
Main stream inlet (Dry air)	T_{main} (K)	1561	450	1561 K = 2350^{o}F
	u_{main} (m/s)	128	10	Uniform
	Tu (%)	5	5	Turbulence intensity
	$\mathrm{Re_l}\times10^{-6}$	1.5	0.062	l=0.2m
Jet inlet (Saturated air)	T_c(K)	644	375	644 K = 700^{o}F
	u_j (m/s)	106	15	Uniform
	Tu (%)	1	1	Turbulence intensity
	$\mathrm{Re_d}\times10^{-3}$	26.8	1.69	
$M=(\rho u)_c/(\rho u)_g$	M	2	1.2	
Outlet	P (atm)	15	1	Constant pressure
Uniformly Cooled wall	q (W/m^2)	2×10^5	2000	Constant heat flux
Conjugate cooling wall	T_{ci} (K)	NA	375	
	h_i (W/m^2-K)		20	
Droplet size	d (μm)	5, 10, 20	5, 10, 20	Uniform
Mist concentration	m_l/m_0 (%)	10, 20	2	
Injection temperature	T_d (K)	472	373	Saturation temperature

Based on experimental results in Guo and Wang (2000), uniform droplet sizes ranging from 5 to 20 μm are simulated. In a real condition the droplet sizes are not uniform, and the results should be a combination of the results bounded by different uniform sizes. Mist is injected uniformly from a surface perpendicular to the jet hole axis and close to the jet inlet. The total trajectories traced are about 10,000. Two different boundary conditions of droplets at walls are simulated: Reflect and Trap. "Reflect" means the droplets elastically bounce off once reaching the wall, while "trap" means "adhere to the wall and evaporate completely." The real situation will be bounded by these two cases as a hybrid condition. Based on wall temperature and droplet parameters, some droplets may stick to the wall and evaporate while others may bounce away from the wall with a partial evaporation.

2.3 Numerical Method

The numerical procedure and methodology in this paper follow those in the studies of Li and Wang (2005a, 2005b), in which the numerical results were qualified by being compared with experimental data. There are 360,000 cells for the 3-D case. Unstructured grids with tetrahedron elements are applied to the coolant passage of the compound-angle jet and a small volume in the main domain close to the jet exit. The rest of domain is meshed to structured but nonuniform grids with hexahedron elements. Figure 2 shows the grids of the coolant passage wall as well as the cooled base surface. Finer grids are generated in the region close to the jet hole and the base wall. For the 2-D slot case, near-wall grids are adapted to examine the grid independence. Adaptation refines the grid in both streamwise and spanwise directions. Detailed discussion of near-wall mesh effect on mist film cooling is referred to the previous study (Li and Wang, 2005b).

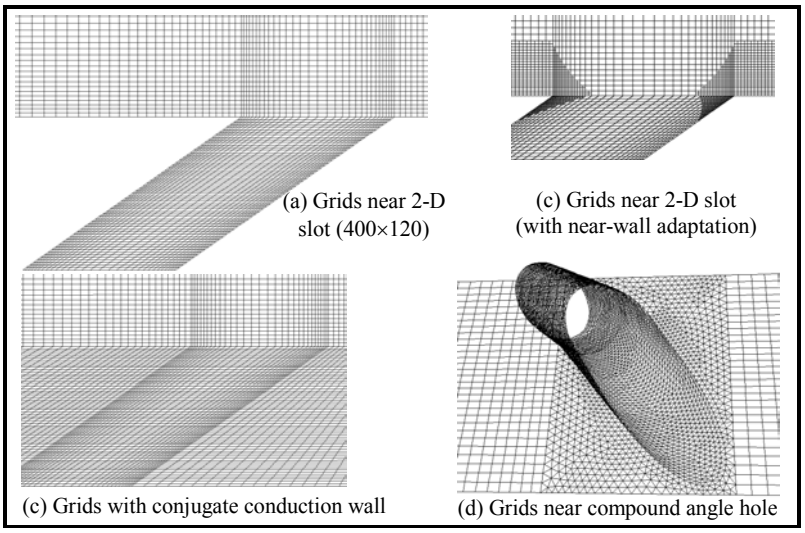

Figure 2 Computational Meshes

Fluent (v. 6.2.16), a commercial software package from Fluent, Inc., is used in this study. The simulation uses the segregated solver, which employs an implicit pressure-correction scheme (Fluent, 2005). Second order upwind scheme is used for spatial discretization of the convective terms and species. Iteration proceeds alternatively between the continuous and discrete phases, and the droplet trajectories are updated every ten iterations in the continuous phase. Results are converged after the specified residuals are met. A converged result renders mass residual of 10^{-4}, energy residual of 10^{-6}, and momentum and turbulence kinetic energy residuals of 10^{-5}. These residuals are the summation of the imbalance for each cell, scaled by the flow rate. Typically, 1000 to 2000 iterations are needed to obtain a converged result, which takes 1~2 hours on a 2.8 GHz Pentium 4 personal computer for 2-D cases and 10-20 hours for 3-D cases.

3. Results and Discussion

3.1 Baseline Case of Mist Film Cooling with the Compound-angle Diffuse Hole

As a baseline case, Figure 3 shows the temperature field and droplet trajectories of the 3-D case with the compound-angle diffuse hole at elevated operational conditions (1561K, 15atm, and 128 m/s) with a blowing ratio of 2, mist concentration at 10%, and 10μm water droplets. The jet flow does not detach from the wall but creates a cold film layer with a thickness of about one jet diameter, which blankets the wall surface quite uniformly. The film coolant flow is not shown but the coolant-affected area can be recognized by the temperature field. The relatively uniform cold blanket with the compound-angle hole can be interpreted by the flow behaviour in the cross-section perpendicular to mainstream direction. As shown in Figure 4, the compound-angle hole provides a well-organized flow close to the wall in downstream region, which makes the coverage uniform in the spanwise direction.

The droplet trajectories are also shown in Figure 3 and these trajectories are only a small fraction of those traced in simulation. It can be seen that rather than following the streamline the droplets move to the top of coolant-affected area, away from the wall and the coolant flow. As found in Wang and Li (2006), this uplift droplet behaviour under the elevated operating conditions downgrades the mist enhancement on film cooling. Even with this downgraded performance, water droplets still play an important role to keep the cooling surface temperature low.

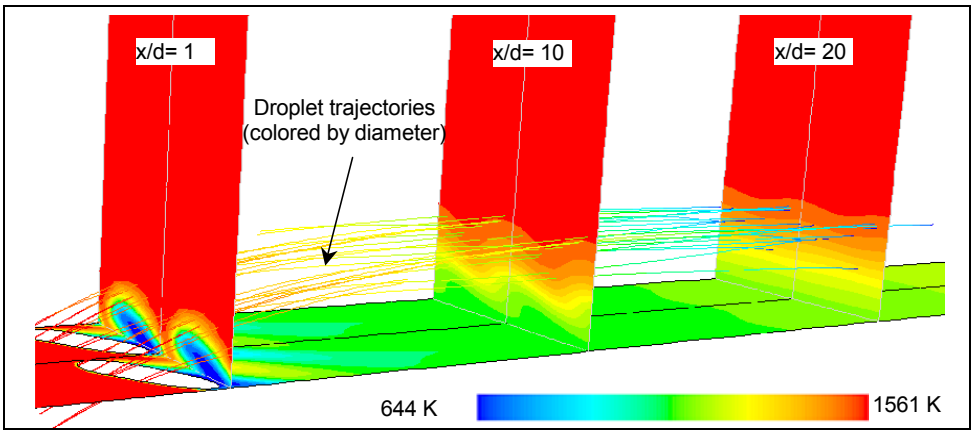

Figure 3 Temperature field and droplet trajectories with the 3-D compound-angle hole.

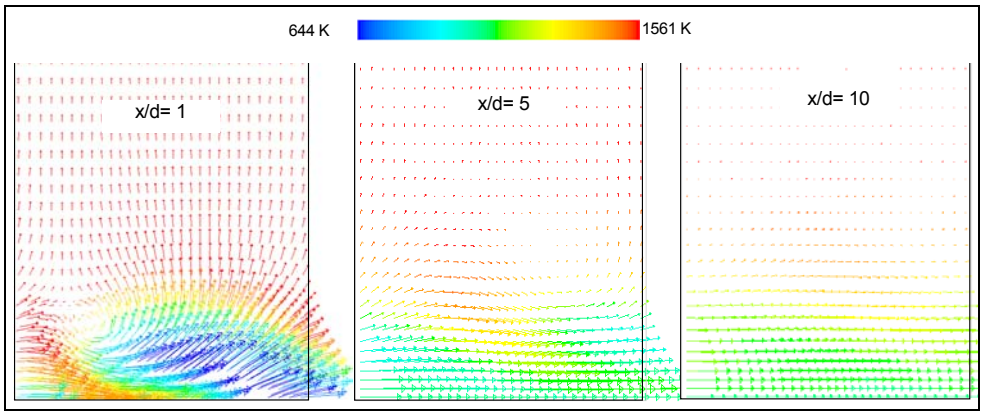

Figure 4 Flow field on planes perpendicular to the mainstream direction
for 3-D compound-angle hole case (Colored by temperature)

The film cooling performance is usually evaluated by the adiabatic film cooling effectiveness, $\eta_a = (T_g\text{-}T_{aw})/(T_g\text{-}T_c)$ with the base wall being insulated. This approach provides a useful reference with a well-controlled boundary condition. However, in the real applications, the cooling of airfoils is usually a conjugate heat transfer accompanied with the internal airfoil cooling. Heat transfer coefficient (h) is usually reported for non-adiabatic cases. The appropriate way to determine the h-value is not straightforward. Two options can be considered: First, it is defined as

$$h_o = q_w''(x)/(T_w\text{-}T_{aw}). \quad (5)$$

This definition provides an appropriate scaling for h-value when different wall cooling or heating fluxes are employed, but it can't fairly show the cooling enhancement induced by mist because T_{aw} of the mist case is lower than the air-only case, so lower T_w of the mist case is not fairly reflected through the h-value. Furthermore, to calculate h_0, an additional computation needs to be conducted to obtain T_{aw} under the adiabatic-wall condition. Therefore, for the convenience of comparing the film cooling performance between air and mist film cooling in this study, a second consideration is given to the local heat transfer coefficient defined as,

$$h = q''(x) / (T_w\text{-}T_g) \quad (6)$$

where the h-value is a function of coolant temperature and wall heat flux in addition to the function of the aerodynamics and surface conditions as conventional heat transfer coefficient is.

Methods have been previously developed to relate the adiabatic cooling effectiveness to the wall heat flux with the intention to keep the h-value as a function of aerodynamics and surface conditions only. For example, Mezger and Mitchell (1966) developed a method to absorb the functionality of T_c into the non-dimensional temperature $\theta = (T_c - T_g) / (T_w - T_g)$ and proved that h is a linear function of θ bounded by two conditions: no heat flux (i.e. $T_w = T_{aw}$) and $\theta = 0$ (i.e., $T_c = T_g$). Eckert (1984) and Choe et al. (1974) developed a superposition method with $h_o = q_w''(x)/(T_w - T_{aw})$ and other h-values with the coolant ejected at the mainstream temperature (i.e. $T_c = T_g$) to determine the actual local heat transfer coefficient as a function of θ. In this paper, we choose to use the definition of Equation (6) because T_c and T_g are fixed for all cases. And thus, the comparison of h-values obtained from Equation (6) is adequate and unique. Furthermore, for conjugated heat transfer boundary condition, two more factors are introduced: internal heat transfer coefficient, h_i, and the internal coolant temperature, T_{ci}. The h-value defined by Equation (6) is the most convenient way for comparing air and mist film cooling performance when both h_i and T_{ci} are also fixed.

The heat transfer result of film cooling with the 3-D compound-angle hole jet is shown in Figure 5 and a constant heat flux is applied to the base cooled wall for this case. To allow readers to compare the differences between the two heat transfer coefficients, both h_o and h are shown in Figure 5. It can be seen that the heat transfer coefficient (h_o), defined by Equation (5), for film cooling with and without mist injection is almost the same, while the heat transfer coefficient (h), defined by Equation (6), is reduced because of mist injection, especially at larger x/d. In this case with the constant heat flux as the boundary condition, a lower h-value indicates a lower surface temperature as shown in Figure 5b. The h-value defined by Equation (6) adequately shows this reduced heat transfer phenomenon; whereas h_0 defined by Equation (5) does not. In the real GT applications, the actual wall temperature reduction is important. The mist film cooling results show the wall temperature reduction increases from 15K to 45K downstream of x/d =15 to 30 in Figure 5b. This is exactly what we really want because the downstream wall is hotter and needs more cooling. The prolonged effect of mist cooling provides this needed service.

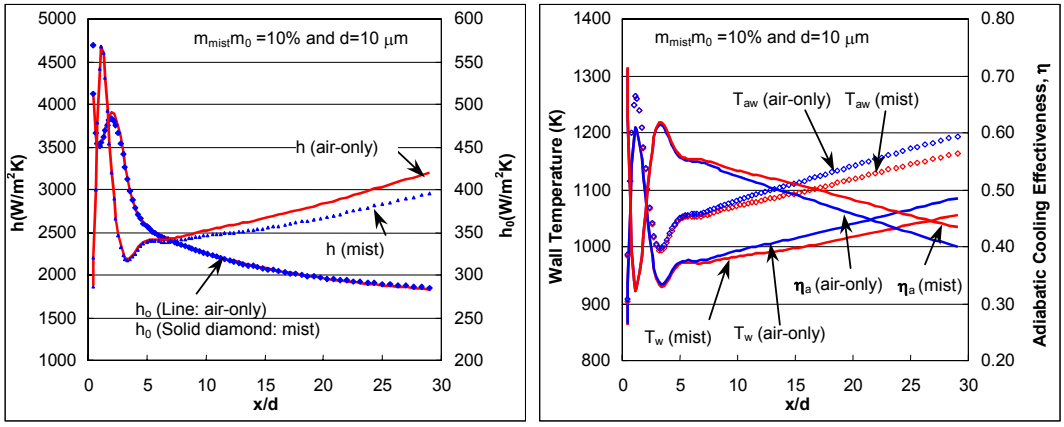

(a) (b)

Figure 5 Heat transfer results of the 3-D case with the compound-angle hole over a uniformly cooled base wall under GT operating condition (15atm and 1561K)

3.2 Effects of Water Droplet Sizes, Mist Concentration, and Droplet-Wall Interaction Model on Film Cooling Performance

Three different water droplet sizes (5, 10, and 20 μm) are simulated. Figure 6a shows the droplet size does not make difference within $x/d < 5$, but the smaller droplets can provide better cooling enhancements (lower h-values and low surface temperatures) downstream of x/d =5. The plausible explanation is that the higher surface to volume ratio of small droplets makes droplet evaporation

more rapidly and effectively than large droplets. In addition, smaller droplet follows the jet flow better and the evaporation occurs more adjacent to the wall as supported by the particle tracing results, which are not shown here due to limited space.

Droplet trajectory of 10% mist concentration (Figure 3) shows that all the droplets evaporate before mainstream exit at x/*d*=30 due to high main flow temperature. By adding more mist up to 20% of the coolant mass flow rate, the result in Figure 6b shows an approximate 10% decrease downstream of x/d = 30 for the h-value, which corresponds to an additional drop of wall temperature of approximately 28K from the 10% mist case and 55K from the air-only case.

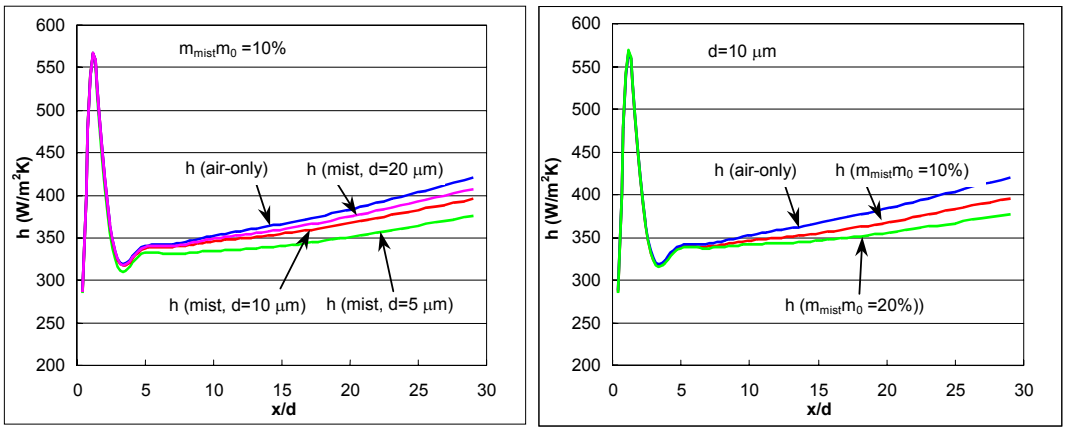

(a) (b)

Figure 6 Effects of (a) droplet size and (b) mist concentration on film cooling with the compound-angle diffuse hole over a uniformly cooled base wall under GT operating condition (15atm and 1561K).

Another factor that may affect mist film cooling is the boundary condition of droplets on the wall (i.e. droplet-wall interactions). In all the cases above, the "reflect" condition is applied, which means the droplet will bounce from the wall elastically. On the opposite end of the extreme case, the "trap" condition assumes the droplets adhere to the wall and evaporate completely once they hit the wall. The true condition shall fall within these two extreme conditions. Both "reflect" and "trap" conditions have been employed and numerical results indicate that these two different conditions produce no difference on heat transfer coefficient. The reason is that only very limited droplets (less than 1%) have a chance to hit the wall in these film cooling cases.

3.3 Heat Transfer of Mist Film Cooling at Low Operational Conditions with a 2-D Slot Jet

Figure 7 shows the results of 2-D case at low operational conditions (1 atm and 450K). Due to mist injection, the heat transfer coefficient (h) decreases for both "reflect" and "trap" boundary conditions. The wall temperature is reduced significantly, and the intensive evaporation with "trap" condition results in a wall temperature below coolant temperature. At low operational conditions, the droplets stay more closely to the wall, following the streamline, which makes the cooling enhancement more effective.

3.4 Effect of Conjugate Heat Transfer on Mist Film Cooling (2-D Slot Jet)

Conjugated wall condition mimics more closely the actual blade cooling with both internal passage cooling and the external film cooling. Figure 8 shows the temperature field of the 2-D film cooling

with conjugated heat transfer. The temperature distribution in the *y*-direction (cross-stream) is relatively uniform in the conduction region. However, the large temperature gradient in the *x*-direction indicates there is a strong axial heat conduction, especially in the proximity of the jet hole. As seen in Figure 8b, the temperature in solid wall at $x/2b$=1 is higher than the local flow temperature. Figure 8 also shows some droplet trajectories. Under the low operating conditions, the droplets stay more closely to the wall, following the streamline. Turbulence random tracking method allows individual trajectory to divert from its time-averaged track and mimics the actual instantaneous turbulence flow fluctuations more adequately.

Figure 9 shows the result of 2-D conjugated heat transfer with internal cooling. Injecting mist lowers the temperature of both internal and external walls. The heat flux transferred to the internal flow with mist injection is gladly found much lower than the air-only case because the reduced internal cooling means more energy will remain in the main flow. The positive heat flux in the neighborhood of jet hole with $x/2b$ <5 indicates a strong axial heat conduction from downstream to upstream due to the large axial wall temperature gradient. It is interesting to see the heat flows back to the mainstream (actually to the jet flow that is cooler than the wall as shown in Fig. 8b), rather than move to the internal cooling flow through the inner wall. Overall speaking, heat flux through the wall is reduced significantly by mist injection. The heat flux losses to the internal flow is almost zero between x/b = 10~25. With the conjugate heat transfer modelling, mist injection can be seen to reduce both the heat transfer coefficient (h), the wall heat flux and the wall temperature.

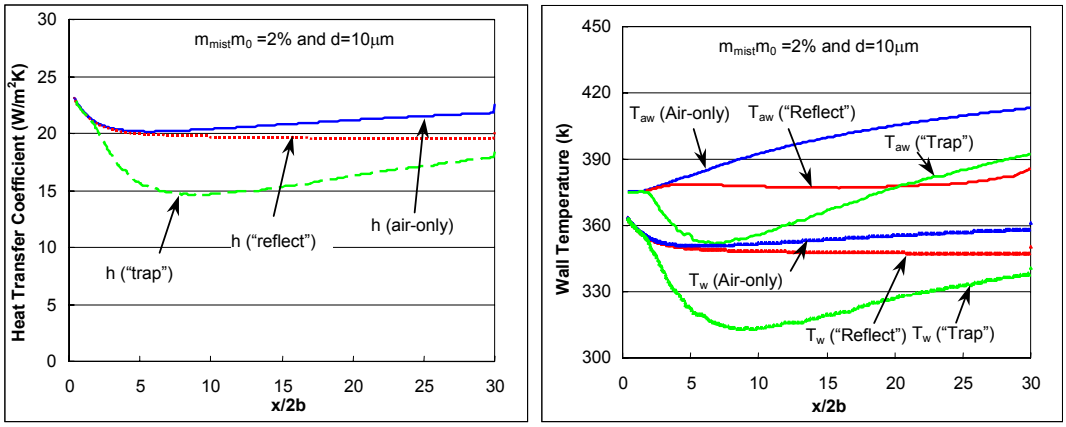

(a) (b)

Figure 7 Heat transfer result of the 2-D slot case at low operational conditions (1 atm and 450K).

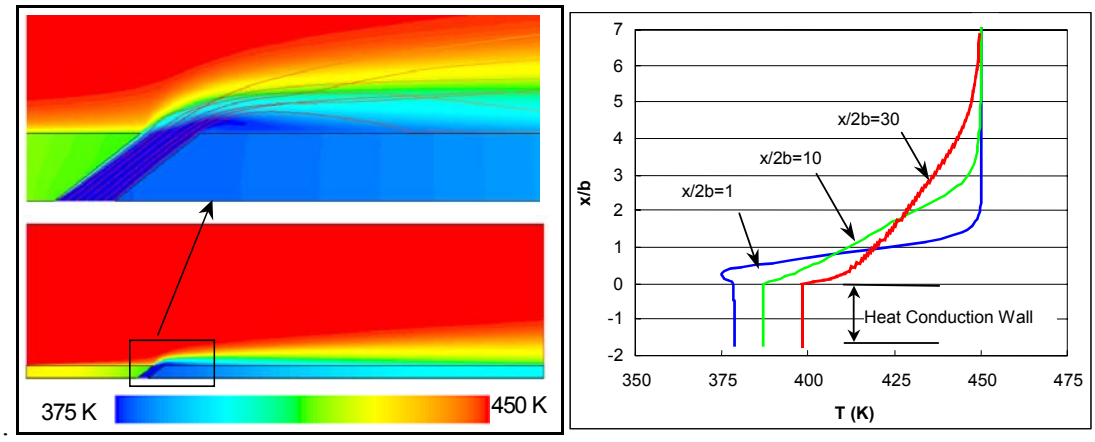

(a) (b)

Figure 8 Temperature distribution of 2-D film cooling with conjugate heat transfer

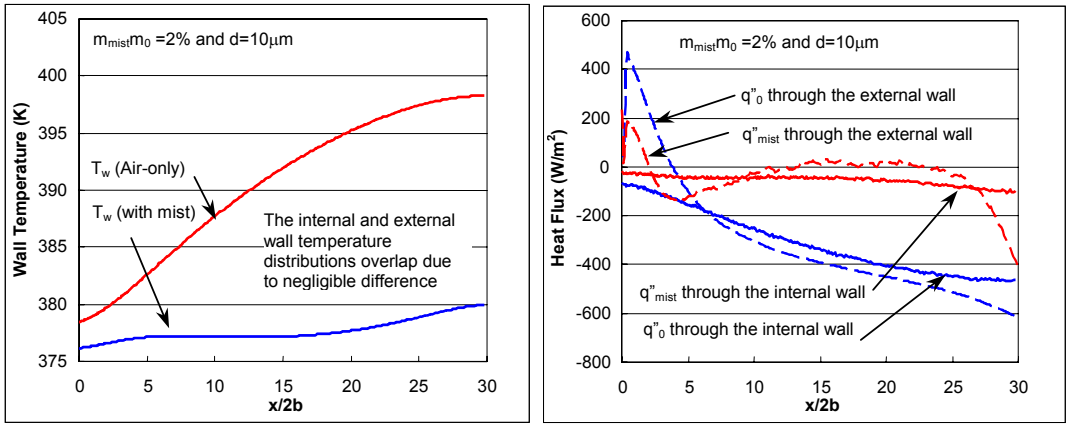

(a) (b)

Figure 9 Heat transfer result of mist film cooling of a 2-D slot jet with a conjugated wall cooling.

4. Conclusions

As an effort to develop an advanced film-cooling scheme, this paper studies heat transfer of film cooling with mist injection. Both low laboratory conditions and realistic gas turbine operating conditions at high temperature, pressure, and Reynolds number (velocity) are considered with different wall heating conditions. The conclusions are:

- Under GT operating conditions with a compound-angle diffuse hole, mist injection reduces the heat transfer coefficient (h) as well as wall temperature, especially at downstream region. The heat transfer coefficient (h_0) has little changes with mist injection.
- Due to a large temperature difference between the main flow and the coolant flow under GT operating conditions, injecting 10% (weight) mist results in an 8% (4 percentage point) reduction of heat transfer coefficient (h) and approximately 40K reduction in wall temperature. Injecting mist provides a prolonged cooling and results to a more effective cooling in the downstream region ($x/d > 15$) where air-only film cooling is less effective.
- Smaller droplets and higher mist concentration result in a stronger surface cooling protection, indicated by a smaller heat transfer coefficient (h) under the same wall heat flux.
- The droplet boundary conditions of "reflect" and "trap" give nearly identical results at GT operating conditions because that most of droplets don't have a chance to hit the wall.
- Under low temperature, pressure, and Reynolds number laboratory conditions, results of 2-D slot jet with conjugate internal cooling shows injecting 2% mist (mass) reduces heat transfer coefficient (h), wall heat flux about 400W/m^2, and wall temperature about 15K.
- Result of conjugated 2-D cases indicates that heat conduction from downstream to upstream along the solid wall is strong. Heat flux through the wall is reduced significantly due to mist injection. The heat flux losses to the internal flow is almost zero between x/b = 10~25. The streamwise heat even conducts back to the film cooling jet flow in the neighborhood of the jet hole within x/b<5.

Acknowledgement

This study is supported by the Louisiana Governor's Energy Initiative via the Clean Power and Energy Research Consortium (CPERC) and administered by the Louisiana Board of Regents.

References

Brittingham, R.A. and Leylek, J. H, 2002, "A Detailed Analysis of Film Cooling Physics: Part IV—Compound-Angle Injection with Shaped Holes," ASME J. Turbomachinery, **122,** pp. 133-145.

Chaker, M., Meher-Homji, C.B., and Mee, M., 2002, "Inlet Fogging of Gas Turbine Engines - Part A: Fog Droplet Thermodynamics, Heat Transfer and Practical Considerations," Proc. ASME Turbo Expo 2002*,* **4**, pp. 413-428.

Choe, H., Kays, W. M., and Moffat, R. J., 1974, "The Superposition Approach to Film-Cooling," Proc. ASME 74-WA/HT-27.

Eckert, E.R. G., 1984, "Analysis of Film Cooling and Full-coverage Film Cooling of Gas Turbines Blades," J. Engineering for Gas Turbines and Power, **106**, pp. 206-213.

Fluent Manual, Version 6.2.16, 2005, Fluent, Inc.

Heidmann, J. D., Rigby, D. L. and Ameri, A. A., 2000, "A Three-Dimensional Coupled Internal /External Simulation of a Film-Cooled Turbine Vane," J. Turbomachinery, **122**, pp. 348-359.

Guo, T., Wang, T., and Gaddis, J. L., 2000, "Mist/Steam Cooling in a Heated Horizontal Tube, Part 1: Experimental System, Part 2: Results and Modeling," J. Turbomachinery, **122**, pp. 360–374.

Jia, R., Sunden, B., Miron, P., and Leger, B., 2003, "Numerical and Experimental Study of the Slot Film Cooling Jet with Various Angles," Proc. ASME Summer Heat Transfer Conf., pp. 845-856.

Kuo, K. Y., 1986*,* Principles of Combustion, John Wiley and Sons, New York.

Li, X. and Wang, T., 2005a, "Simulation of Film Cooling Enhancement with Mist Injection," Accepted for publication in ASME Journal of Heat Transfer, also in Proc. ASME Turbo Expo 2005 (GT2005-69100), Reno, Nevada, June 6-9, 2005

Li, X, and Wang, T, 2005b, "Effects of Various Modeling on Mist Film Cooling," Proc. ASME Int. Mechanical Eng. Congress and Exhibition (IMECE 2005-81780), Orlando, Florida, Nov. 2005.

Martini,P., Schulz ,A. and Bauer, JH, 2005, "Film Cooling Effectiveness and Heat Transfer on the Trailing Edge Cut-Back of Gas Turbine Airfoils With Various Internal Cooling Designs," Proc. ASME Turbo Expo 2005, Nevada, USA, June 6-9.

Mayhew, J. E., Baughn, J. W., and Byerley, A. R., 2004, "Adiabatic Effectiveness of Film Cooling with Compound Angle Holes-The Effect of Blowing Ratio and Freestream Turbulence," ASME J. Heat Transfer, **126**, pp. 501-502.

Metzger, D. E., Carper, H.J., and Swank, L. R., 1968, "Heat Transfer with Film Cooling Near Nontangential Injection Slots," J. Engineering for Power, Vol. 90, pp. 157-163.

Petr, V., 2003, "Analysis of Wet Compression in GT's," Energy and the Environment – Proc. the Int. Conf. on Energy and the Environment, **1**, pp. 489-494.

Ranz, W. E. and Marshall, W. R. Jr., 1952, "Evaporation from Drops, Part I," Chem. Eng. Prog., **48**, pp. 141-146.

Rutledge, J. L., Robertson, D., and Bogard, D. G., 2005, "Degradation of Film Cooling Performance on a Turbine Vane Suction Side Due to Surface Roughness," Proc. ASME Turbo Expo 2005, Nevada, USA, June 6-9.

Tyagi, M. and Acharya, S., 2003, "Large Eddy Simulation of Film Cooling Flow from an Inclined Cylindrical Jet," ASME J. Turbomachinery, **125**, n. 4, pp. 734-742.

Wang, T. and Li, X, 2006, "Simulation of Mist Film Cooling at Gas Turbine Operating Conditions," Proc. ASME Turbo Expo 2006 (GT 2006-90742), Barcelona, Spain